Characterize human mobility in Nigeria during flooding season and its impact in shaping the spread of Covid-19

Kailun Liu
Department of Civil and Environmental Engineering
Villanova University
Villanova, United States
kliu03@villanova.edu

Xin Wu
Department of Civil and Environmental Engineering
Villanova University
Villanova, United States
xin.wu@villanova.edu

Lele Zhang
Department of Civil and Environmental Engineering
Villanova University
Villanova, United States
lzhang02@villanova.edu

Chenfeng Xiong*
Department of Civil and Environmental Engineering
Villanova University
Villanova, United States
chenfeng.xiong@villanova.edu

2024 IEEE Global Humanitarian Technology Conference (GHTC) | 979-8-3503-7734-7/24/$31.00 ©2024 IEEE | DOI: 10.1109/GHTC62424.2024.10771507

***Abstract*— In 2020, Nigeria suffered from both intensified flooding seasons due to climate change and the onset of the COVID-19 pandemic. This study investigates the interconnected dynamics of flooding, human mobility, and COVID-19 transmission in Nigeria during the 2020 flooding season. Utilizing a two-stage spatial panel econometric model, the study incorporates data from satellite imagery, mobility tracking, and regional COVID-19 case reports. The results show that flooding severity, along with heavy rainfall, significantly impacts daily human mobility, which in turn influences the spread of COVID-19. These findings highlight the complex challenges at the intersection of natural disasters and public health, underscoring the need for a national-scale flood management plan in developing countries such as Nigeria.**

Keywords—flood, human mobility, climate change, COVID-19

I. INTRODUCTION

The interplay between natural disasters and infectious diseases, intensified by the effects of climate change, presents a complex public health challenge that demands a deep understanding and detailed examination of the correlations between those factors. In Nigeria, seasonal flooding, exacerbated by the effects of climate change, stands as a significant natural disaster. It affects large areas of the country, disrupting lives, and exacerbating public health concerns [1]. The 2020 flooding season, one of the most severe in recent memory, highlighted the urgency of addressing this issue. The Nigeria Hydrological Services Agency (NHSA) reported that the floods impacted all 36 states, including the Federal Capital Territory (FCT), 349 Local Government Areas (LGA), and 2,353,647 people, resulting in 69 fatalities [2]. This phenomenon became particularly critical considering the global outbreak of the COVID-19 pandemic in 2020, where human mobility could influence the spread and management of the disease [3]. This paper aims to characterize human mobility in Nigeria during the 2020 flooding season and its impact in shaping the spread of COVID-19, offering insights into the challenges and opportunities for public health interventions in such complex scenarios.

Nigeria, positioned on the western coast of Africa, spans a vast geographical area of approximately 923,800 sq. km, home to about 200 million people which rank the first in African countries [4]. It's a country of rich diversity, bordered by the Republic of Cameroon to the east, the Republic of Niger to the north, the Republic of Benin to the west, and the Atlantic Ocean to the south. This strategic location gives Nigeria with a variety of climatic conditions and vegetation belts, from coastal wetlands and deltas in the south to highlands and plateaus in the north, divided by the Niger and Benue rivers. The country's climate varies significantly, influenced by its distance from the Atlantic coast, with areas within 100 km of the coast experiencing the Köppen's Af humid tropical climate, while regions further inland exhibit the Köppen's Aw1 wet and dry climate type [2]. These geographical and climatic characteristics significantly shape Nigeria's vulnerability to natural disasters, particularly flooding. Annual flooding impacts various parts of the country, especially the coastal and riverine areas, driven by heavy rainfall, dam releases, lack of clear disaster management policies and inadequate urban drainage [5]. The situation is further complicated by the exacerbating effects of climate change, leading to more severe and unpredictable flooding events [6].

Flood mapping and modeling typically require a large amount of accurate and up-to-date data, which is often not readily available in developing countries such as Nigeria [7]. However, with the advancement of remote sensing technology and GIS methods, these tools are becoming increasingly popular and accessible for flood mapping and modeling [8]. Reference [9] employed GIS methods to study land cover changes in flood-prone areas of Igbokoda town in Ondo, Nigeria. The Niger-Benue River basin area was analyzed using watershed analysis by [10] to identify areas at high risk of flooding. The ArcView GIS package was used by [11] to identify vulnerable areas and study the impact of waterborne diseases following floods. However, there are still gaps in research, particularly regarding the lack of national-scale flood mapping needed to perform

2024 IEEE Global Humanitarian Technology Conference (GHTC)

hazard risk and vulnerability assessments in Nigeria that help to provide a synchronized flood action plan [12].

This research aims to close the gap by developing a two-stage spatial panel econometric model that captures the spatial and temporal interplay between flooding severity, human movement, and the spread of COVID-19 at the national scale. The framework of the model is showcased in Fig. 1. This model also considers variations in demographic characteristics within the study area, which encompasses 773 LGAs in Nigeria, during the period from April to October 2020. A detailed map of the study area is presented in Fig. 2. The model integrates data from four key resources: (1) human mobility data collected and aggregated through mobility devices, (2) flooding severity assessed through satellite imagery, (3) daily COVID-19 case numbers, and (4) sociodemographic variables at both LGA and state levels.

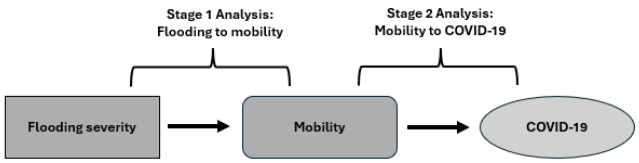

Fig. 1. Framework of the two-stage spatial panel data econometric model at national level.

Fig. 2. Study area of the two-stage model at national level.

II. Data

A. COVID-19

The first case in Nigeria was reported on the 27th of February 2020, and by the end of 2020, there were approximately 83,000 cases with more than 1,200 deaths [13]. The COVID-19 data utilized in this research is aggregated at the subnational (state) level. The original source of the data is the Nigeria Centre for Disease Control, which was further collected and processed by Humanitarian Emergency Response Africa (HERA). In this study, daily new COVID-19 case number per 1,000 people is used as the metric to measure the spread of COVID-19.

B. Flooding

To assess the severity of flooding events accurately, this research utilizes the powerful remote sensing capabilities of Google Earth Engine (GEE), which grants easy access to an extensive variety of satellite imagery to generate Flood Inundation Mapping (FIM). Sentinel-1 satellite data are applied in this study. Sentinel-1 is served as a part of the Copernicus program by the European Space Agency (ESA). The data are collected through Sentinel-1's constellation, comprising Sentinel-1A and Sentinel-1B satellites, equipped with C-band Synthetic Aperture Radar (SAR) [14].

Furthermore, the Ground Range Detected (GRD) products for the Sentinel-1 satellite with 10m resolution were used. The GRD products contain imagery data specifically processed to minimize speckle noise and enhance the quality of the intensity images. The selection criteria for the imagery included the Interferometric Wide swath mode ('IW') suitable for land monitoring, dual 'VH' and 'VV' polarization for superior water surface detection, and an 'ASCENDING' pass direction to ensure consistency in observation geometry.

An algorithm for estimating flooded areas, similar to the one described by [15] was then used to observe and calculate the extent of reliably flooded areas. First, the algorithm used differential analysis to apply SAR backscatter values between dry and flooding seasons. Areas with a threshold value of 1.47 were selected as potential flooded areas. Then the permanent and seasonal water needed to be removed from the potential flooded area. The algorithm used the JRC Global Surface Water Mapping dataset's 'seasonality' measure to mask out water areas where water presence was detected for four or more months of the year [16]. In the next step, a Digital Elevation Model (DEM) from HydroSHEDS was used to detect areas with a slope above 5 percent. These areas were then considered too steep for floodwater to accumulate and thus masked out. Lastly, a connectivity filter for more than 30 connected pixels was applied to ensure the spatial continuity of identified flood waters, thus enhancing the accuracy of the flood mapping efforts.

A demonstration of Sentinel-1 AWS-IW-VVVH imagery in Nigeria, captured between July 1st and July 15th, 2020, is showcased in Fig. 3. The imagery was plotted using the EO Browser.

Fig. 3. Sentinel-1 AWS-IW-VVVH RGB ratio imagery for Nigeria from July 1st to July 15th, 2020.

In this research, the flooding area was collected and calculated for each LGA within the study region. Due to the satellite's circular motion around the Earth, data collection required a certain period of time, which, for this study, was set at 15-day intervals during April and October 2020. A total of 14 flood maps were generated for this study.

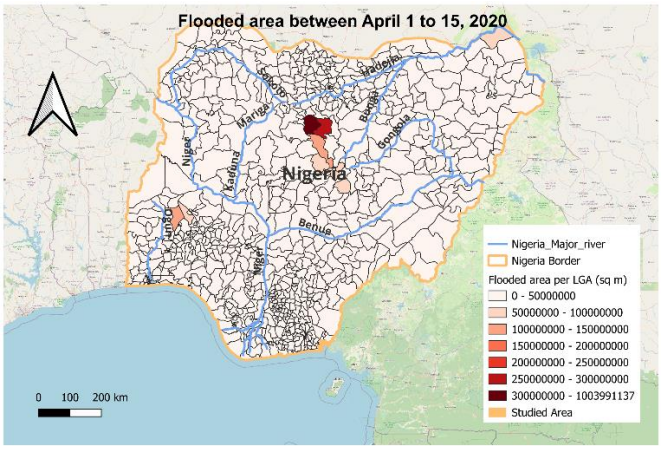

(a)

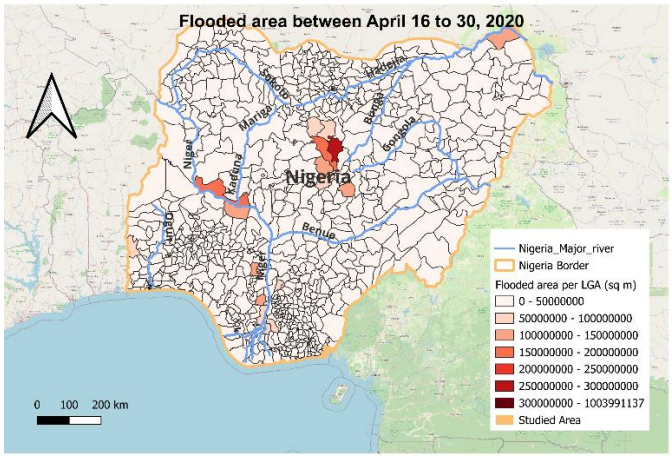

(b)

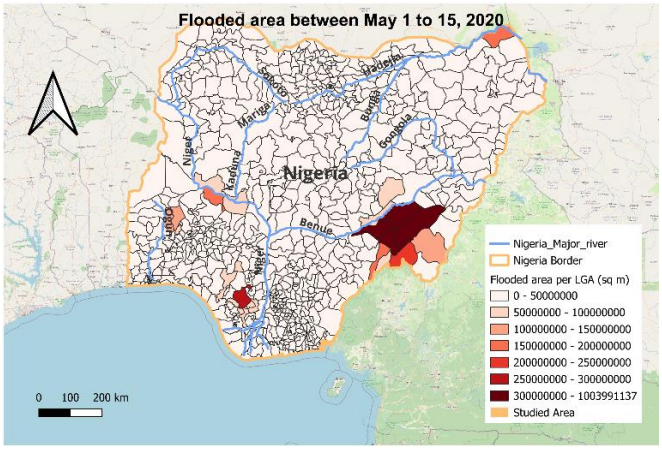

(c)

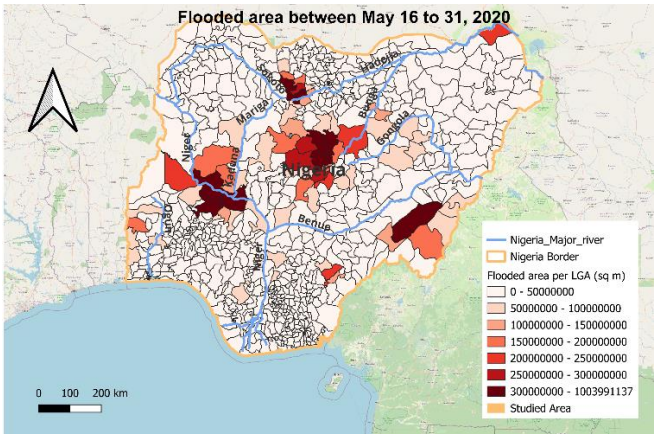

(d)

Fig. 4. Flooded area for each LGA within the study area (a) between April 1 to15, (b) between April 16 to 30, (c) between May 1 to 15, (d) between May 16 to 31.

However, using only the flood area as a metric to measure the extent of flooding in each LGA can introduce significant bias due to the large differences in LGA size and the extent of permanent water areas. For example, Fig. 4 shows that the southern LGAs had observed larger flooding areas, with some exceeding 1000 sq. km. However, this did not necessarily indicate more severe flooding in those LGAs. To address this issue, a variable called 'flooding severity' was created to minimize bias by considering the ratio between the LGA area and the flood area, thus providing a more accurate representation of the flooding situation in each LGA. The formula for calculating flooding severity is shown in (1):

$$Flooding\ severity\ = \frac{Flooding\ area}{LGA\ area - Permanent\ water\ area} \quad (1)$$

Flooding severity at the LGA level was calculated from June 1st to July 31st, 2020, in the study area. The detailed values are shown in Fig. 5. From Fig. 5, it can observe high flooding severity in the northern region of the study area, like

the pattern presented in Fig. 4, which was plotted using only the flooding area data. However, the flooding severity map also showcases that the flooding patterns gradually shift from the northern region to the central LGAs and then move to some of the LGAs near the river sheds in the southern part of the study area.

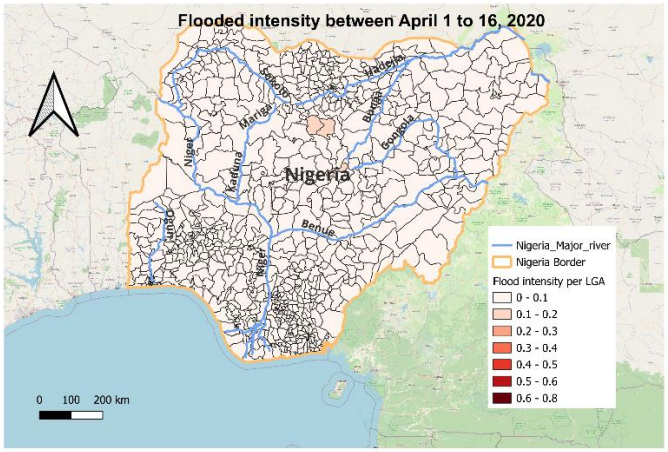

(a)

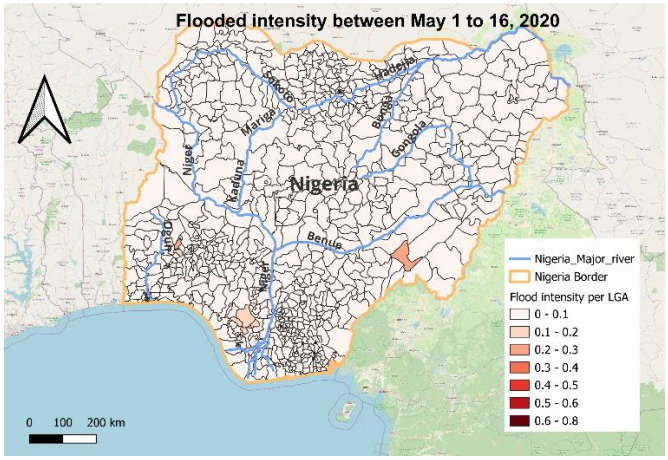

(b)

Fig. 5. Flooding severity mapping (a) from April 1st to 16th and (b) from May 1st to 16th..

C. Human mobility data

The human mobility data utilized in this analysis were sourced from the Human Mobility Data Repository (https://github.com/villanova-transportation/Human-Mobility-Data-Hub). This data, which measures daily human mobility metrics, was gathered through third-party providers using location-based data. For more detailed information, please refer to the paper by [17]. In our analysis, the primary metric of human mobility employed is the daily number of trips per person, serving as an effective indicator of the region's travel behavior.

D. Rainfall data

Daily rainfall data is collected using the ERA5 dataset provided by the fifth-generation European Centre for Medium-Range Weather Forecasts (ECMWF). This data set combines model data with observations from around the world. Through data assimilation, ERA5 provides a consistent global dataset, including information on daily total precipitation (TP) and daily temperature of air at 2m above the surface (T2m).

Fig. 6 shows the gridded weather points that cover the entire area of Nigeria, with orange squares representing the centroids of LGAs. To obtain rainfall data for each LGA, we map the corresponding weather points onto the LGAs. For LGAs that contain weather points, we calculate the mean values of these points for our observations. For smaller LGAs without encompassing weather points, we identify the gridded square containing their centroid. In these cases, we take the mean value of the four weather points within that square to use as our observation.

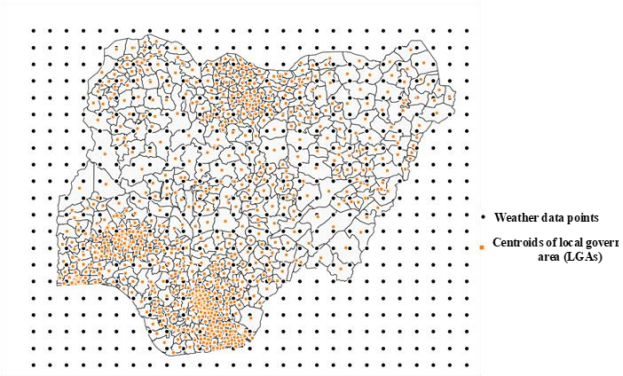

Fig. 6. Gridded weather points from ERA5 and centroids of LGAs.

E. Socio demographic

Previous research has demonstrated that demographic variables, particularly characteristics of vulnerable populations such as age, income, and ethnicity, significantly influence the spread of COVID-19 within a region [19, 20]. This analysis utilizes socio-demographic variables at both the state and LGA levels from various sources. For the state level, the majority of the data come from the Nigeria Data Portal (https://nigeria.opendataforafrica.org), which offers over 30 unique variables ranging from poverty and income to education and demographics. However, the portal has its limitations, including outdated data and missing information for some underdeveloped states [21]. For our analysis, we selected variables with the most recent updates and ensured availability for each state in the study area. Selected variables include GDP per capita, population density, percentage of age groups, and percentage of the population using improved drinking water sources. Point of Interest (POI) data, including schools, markets, churches, health facilities, and more, are collected from the GRID3 data hub (https://grid3.org). These POI data are then aggregated at the Local Government Area (LGA) level

and State level. There are also other available POI data from mapping services such as OpenStreetMap. However, these data can come from various sources, including open communities, making it difficult to verify the quality of the POI data when the study area is at a national scale. On the other hand, GRID3, which is collected from government sources, includes labels indicating whether the POIs are still in use. Therefore, for this study, only GRID3 data is included.

A detailed description of the variables is presented in Table I.

TABLE I. DESCRIPTION OF VARIABLES USED IN THE MODEL.

Variables	Description
Trips per person	Number of trips made per person per day
Flooding severity	Flooding severity metric
Weekend	Weekend index: 0: weekday 1: weekend
Rainfall	Daily total rainfall (mm)
Temperature average	Daily temperature of air at 2m above the surface of land, sea or inland waters (k)
Male	Male population percentage
Socio index	Average socioeconomic vulnerability score per LGA, from a 1 to 5 scale, with 5 indicating the highest level of vulnerability
Health facility density	Number of health facilities per sq.km
Church density	Number of churches per sq.km
Market density	Number of markets per sq.km
Mosques density	Number of mosques per sq.km
Age 65 years and older	Age 65 years and older population percentage
Age 18 and younger	Age 18 and younger population percentage
COVID cases per 1000 people	Daily new COVID-19 cases per 1000 people
Population density	Population density (ppsq.km)
Fully immunization	Full immunization percentage for children between 12 to 23 months
GDP	GDP Per Capital
Sanitation	Population percentage use of improved sanitation facilities
Unemployment rate	Unemployment rate
Income inequality	Income inequality index
Child labor	Chile labor percentage

III. METHODOLOGY

The data collected for this study contains both time-series observations and observations across different spatial units at the same time point, which is considered to be spatial panel data [22]. When dealing with this type of data, an ordinary least squares (OLS) model can be biased and lead to false interpretations due to the assumption of independent normally distributed residual [26] and ignorance of existing spatial autocorrelation [23-25]. For this reason, a spatial panel econometric model is selected for this analysis due to the models being able consider variability both in time and space.

A. Spatial analysis

Before the spatiotemporal analysis, a spatial analysis is needed to create two weight files for the study area for each stage of the analysis. In this study Queen's first-order contiguity [27] is used to determine the neighboring spatial unit for each unit in the study area. Then LM-H one-sided joint test is performed on a linear regression model with the same variables to check if spatial autocorrelation including spatial lag and spatial error exists in the dataset [28]. The null hypothesis for this test is that there is no spatial autocorrelation in the data. If the null hypothesis is rejected, a spatial panel model is needed.

B. Spatial temporal analysis

Maximum likelihood estimation spatial panel model with random affect is used for the two-stage model. This type of model is able to consider the temporal autocorrelation of the dependent variable, along with capabilities for random spatial and temporal effects. The 'splm' package in R is utilized for the model building process. For this study, spatial lag plus various error terms including spherical errors (OLS), Anselin-Baltagi type spatial autoregressive error (SEM), Kapoor, Kelejian and Prucha-type spatial autoregressive error model with spatially correlated random effects (SEM2), random affect (RE) and serially correlated remainder errors (SR) are considered to determine the best-fitted model [29]. The model unfolds in two stages: the initial analysis at the Local Government Area (LGA) level, transitioning to a state-level analysis due to the COVID-19 data in Nigeria is only available at state level at the second stage. The detail dependent variables used and level of analysis for each stage is presented in Table II.

TABLE II. BALTAGI, SONG AND KOH LM-H ONE-SIDED JOINT TEST RESUTL FOR TWO-STAGE MODEL.

Stage	Dependent variable	Level of analysis
Stage one	Trips per person	LGA
Stage two	COVID cases per 1000 people	State

IV. RESULT

A. Temporal analysis

Weight files are created for both stage one and stage two of the analysis. The connectivity maps for both stages are presented in Fig. 7.

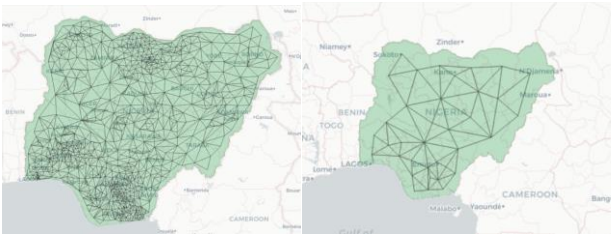

(a) (b)

Fig. 7. Connectivity map for (a) stage one at LGA level and (b) stage two at state level.

Two separate LM-H one-sided joint tests were performed to test for the existence of spatial autocorrelation with the result presented in Table III. The results, with LM-H values of 208.07 for stage one and 483.27 for stage two, indicate significant spatial autocorrelation in the fitted linear regression model at both stages. Therefore, a spatial panel model is needed to properly address the spatial autocorrelation.

TABLE III. BALTAGI, SONG AND KOH LM-H ONE-SIDED JOINT TEST RESUTL FOR TWO-STAGE MODEL.

Stage	Alternative hypothesis	LM-H	P-value
Stage one	Spatial autocorrelation	208.07	< 2.2e-16
Stage two	Spatial autocorrelation	483.27	< 2.2e-16

B. Spatial temporal analysis

1) Model Parameters and Fitted Scores

The model parameters and fitted scores are presented in Table IV. The goodness of fit of the model is determined by the values of the Akaike Information Criterion (AIC) and the Bayesian Information Criterion (BIC). For both stages, the spatial panel model with spatial lag, spatially correlated random effects, and random effects is selected because it has the lowest AIC and BIC scores compared to other options.

TABLE IV. MODEL PAPRAMETER AND FITTED SCORES FOR THE TWO STAGE MODEL.

	AR(1) serial correlation	Error type	Spatial Lag	AIC (stage one)	BIC (stage one)	AIC (stage two)	BIC (stage two)
1	False	OLS	False	130729.6	130889.6	-68214.41	-68123.95
2	False	OLS	True	130334.4	130494.3	-71426.49	-71336.04
3	False	SEM	True	130308.3	130458.3	-71451.91	-71361.46
4	True	SRRE	True	117415.5	117565.4	-71701.24	-71617.74
5	False	RE	False	117734.1	117894.1	-71694.97	-71604.51
6	False	RE	True	117249	117408.9	-71773.39	-71682.93
7	**False**	**SEM 2RE**	**True**	**117089.6**	**117249.5**	**-71849**	**-71758.59**

Noted if the spatial lag is false then a temporal lag term for the dependent variable is manually added in the equation.

2) Stage one result

The coefficient estimates result for stage one model is shown in Table V. From the result, we find that flooding severity was positively associated with the daily number of trips per person, implying that increased flooding might lead to more trips. This is likely due to the long observation period (every 15 days) for flood data collection, which may include with days when people are evacuating or securing supplies. The combined effects of flooding severity and daily rainfall was negatively associated with trips, intensifying the inhibitive effect of bad weather on travel.

For weather-related variables, rainfall and temperature were both negatively associated with the daily number of trips per person, indicating that increased rainfall and extreme temperatures discourage travel. On the other hand, LGAs with a high percentage of the population aged 65 years and older, as well as those aged 18 years and younger, demonstrated significant negative associations with daily trips. This indicates that these vulnerable demographic groups undertake fewer daily trips during the flooding season.

For POI related variables, Both health facility and church density showed no significant effects or minor associations, indicating these locations have less influence on daily travel patterns. A strong negative association for marketplace density suggested that higher concentrations of marketplaces might decrease the need for longer or additional trips.

There is also a significant positive estimate for the spatial autoregressive coefficient, which reveals that there is a positive correlation between the daily number of trips in each Local Government Area (LGA) and its neighboring LGAs. This indicates a spillover effect, where areas with a high number of trips tend to be clustered together, as do areas with a low number of trips. In other words, if an LGA experiences high daily trip mobility pattern, its neighboring LGAs are also likely to show similar patterns of high mobility.

TABLE V. ESTIMATION RESULT OF STAGE ONE MODEL FOR FLOODING IMPACT ON DAILY NUMBER OF TRIPS PER PERSON.

Variable	Estimate	Std. Error	Pr (>|t|)
(Intercept)	1.7991060	0.2483644	4.362e-13 ***
Trips per person 1 day lag	0.2529025	0.0023940	< 2.2e-16 ***
Weekend	-0.0175163	0.0018980	< 2.2e-16 ***
Flooding intensity	0.0146597	0.0078672	0.0624083 .
Rainfall	-0.0044177	0.0012348	0.0003465 ***
Temperature	-0.0091673	0.0013920	4.531e-11 ***
Population density	0.0010677	0.0093982	0.9095528
Socio index	-0.0385985	0.0060376	1.626e-10 ***
Health facility density	0.0067752	0.0118445	0.5673147
Marketplace density	-0.2646356	0.0593345	8.193e-06 ***

Mosques density	0.0716370	0.0308043	0.0200425 *
Church density	-0.0300818	0.0164320	0.0671480 .
Age 65 years and older	-1.7509324	0.7891848	0.0265099 *
Age 18 and younger	-1.1277432	0.1893812	2.603e-09 ***
Male	-1.3096795	0.3908685	0.0008061 ***
Flood intensity and rainfall	-0.0178684	0.0047275	0.0001571 ***
Spatial autoregressive coefficient	0.334862	0.011286	< 2.2e-16 ***

Significant. codes: 0 '***' 0.001 '**' 0.01 '*' 0.05 '.' 0.1 ' ' 1

3) Stage two result

The coefficient estimates result for stage two model is shown in Table VI. From the result, coefficient for COVID cases per 1000 people (1-day lag) is significantly positive, indicating a strong day-to-day persistence in case counts. This highlights the contagious nature of the virus and the impact of existing caseloads on subsequent infection rates.

Health facility density and GDP show positive relationships with case counts, suggesting areas with higher health facility density and more medical resources are report more cases, potentially due to more available testing kit and surveillance in the health facilities.

Population percentage using improved sanitation facilities shows a negative effect on daily COVID-19 cases, indicating a potential mitigating impact on the spread of the virus.

Interestingly, the result shows a significant negative correlation between trip number 10 days ago to the daily covid-19 cases. In response to rising COVID-19 cases, the Nigeria government has impose restrictions such as lockdowns, curfews, or travel bans in the high COVID case areas. These measures would directly decrease mobility, leading to fewer trips.

The study also reveals that LGAs with higher populations aged 65 and older, as well as areas with significant child labor, report fewer COVID-19 cases. This discrepancy is likely due to underreporting and lack of testing in those underdeveloped regions.

TABLE VI. RESULT OF STAGE TWO MODEL FOR MOBILITY IMPACT ON DAILY NUMBER OF COVID-19 CASES.

Variable	Estimate	Std. Error	Pr (>|t|)
(Intercept)	2.8210e-03	1.0414e-03	0.0067528 **
COVID-19 cases 1 day lag	3.1194e-01	9.7151e-03	< 2.2e-16 ***
Trips per person 10 day lag	-7.9044e-04	1.3953e-04	1.47e-08 ***
Flooding intensity	-5.8983e-04	2.5849e-04	0.0224990 *
Rainfall	4.7355e-05	2.3054e-05	0.0399637 *
Temperature	-1.3004e-04	3.4915e-05	0.0001957 ***
Health facility density	5.8462e-04	2.7830e-04	0.0356725 *
Age 65 years and older	-3.8269e-02	1.8928e-02	0.0431908 *
GDP	5.1056e-04	1.4883e-04	0.0006025 ***
Child labor	-3.3392e-04	1.2321e-04	0.0067242 **
Sanitation	-1.1459e-05	8.2495e-06	0.1648194
Unemployment rate	-2.3114e-06	1.2862e-05	0.8573885
Income inequality	1.4066e-04	2.4543e-03	0.9542981
Spatial autoregressive coefficient	0.40643	0.02521	< 2.2e-16 ***

Significant. codes: 0 '***' 0.001 '**' 0.01 '*' 0.05 '.' 0.1 ' ' 1

V. DISSCUSSION AND FUTURE WORK

Flooding in Nigeria is a comprehensive national-level problem that is worsening due to the impact of climate change. By leveraging modern technology and models, including satellite imagery, location-based data, and econometric spatial models, this study provides a possible solution to build a national-scale flood mapping analysis to identify the impacts of flooding on human mobility and disease transmission.

The analysis reveals that flooding severity can lead to increased trips due to evacuation and securing supplies, while adverse weather conditions like heavy rainfall and extreme temperatures deter travel. Vulnerable populations, such as the elderly and young children, are particularly affected, undertaking fewer trips during flooding. This underscores the need for targeted support for these groups during extreme weather events. The study also highlights the varying influences of different points of interest (POI) on travel patterns, with marketplaces reducing the need for additional trips. Moreover, the spatial spillover effect observed in travel patterns across neighboring LGAs indicates that mobility patterns are not isolated but rather interconnected. This finding suggests that regional coordination in response strategies is crucial.

The second stage model emphasizes the persistence of COVID-19 cases and the role of health facility density and GDP in reporting higher case counts, likely due to better testing capabilities. This underscores the importance for policymakers to consider the availability of health resources when designing disease-related policies. Areas with better health infrastructure are more capable of detecting and reporting cases, which might lead to apparent higher case counts. Policymakers should also consider the disparities and ensure equitable distribution of testing resources and healthcare services to accurately monitor and address the spread of the virus in all areas.

Several future works can be added to enhance this research. First, the accuracy of the flood mapping can be improved by providing ground truth data. An accuracy assessment can then be performed to aid in more precise validation and calibration of the flood observation methods and parameters used.

Additionally, a supplementary model that leverages rainfall data can be added to address the time gaps in satellite observations.

REFERENCES

[1] Echendu, A. J. (2020). The impact of flooding on Nigeria's sustainable development goals (SDGs). Ecosystem Health and Sustainability, 6(1), 1791735.

[2] Nigeria Hydrological Services Agency. (2021). Annual Flood Outlook 2021. Nigeria Hydrological Services Agency. https://nihsa.gov.ng/wp-content/uploads/2021/05/2021-AFO.pdf

[3] Xiong, C., Hu, S., Yang, M., Luo, W., & Zhang, L. (2020). Mobile device data reveal the dynamics in a positive relationship between human mobility and COVID-19 infections. Proceedings of the National Academy of Sciences, 117(44), 27087-27089.

[4] United Nations Development Programme. (2020). Climate change adaptation. https://www.adaptation-undp.org/hazards-addressed/disease

[5] Mashi, S. A., Oghenejabor, O. D., & Inkani, A. I. (2019). Disaster risks and management policies and practices in Nigeria: A critical appraisal of the National Emergency Management Agency Act. International journal of disaster risk reduction, 33, 253-265.

[6] Okon, E. M., Falana, B. M., Solaja, S. O., Yakubu, S. O., Alabi, O. O., Okikiola, B. T., ... & Edeme, A. B. (2021). Systematic review of climate change impact research in Nigeria: implication for sustainable development. Heliyon, 7(9).

[7] Nkwunonwo, U. C., Whitworth, M., & Baily, B. (2020). A review of the current status of flood modelling for urban flood risk management in the developing countries. Scientific African, 7, e00269.

[8] Pourghasemi, H. R., & Gokceoglu, C. (Eds.). (2019). Spatial modeling in GIS and R for earth and environmental sciences. Elsevier.

[9] Adewumi, J. R., Akomolafe, J. K., Ajibade, F. O., & Fabeku, B. B. (2016). Application of GIS and remote sensing technique to change detection in land use/land cover mapping of Igbokoda, Ondo State, Nigeria. Journal of Applied Science & Process Engineering, 3(1).

[10] Akinbobola, A., Okogbue, E. C., & Olajiire, O. O. (2015). A GIS based flood risk mapping along the Niger-Benue river basin in Nigeria using watershed approach. Ethiopian Journal of Environmental Studies and Management, 8(6), 616-627.

[11] Dalil, M., Mohammad, N. H., Yamman, U. M., Husaini, A., & Mohammed, S. L. (2015). An assessment of flood vulnerability on physical development along drainage channels in Minna, Niger State, Nigeria. African Journal of Environmental Science and Technology, 9(1), 38-46.

[12] Komolafe, A. A., Adegboyega, S. A. A., & Akinluyi, F. O. (2015). A review of flood risk analysis in Nigeria. American journal of environmental sciences, 11(3), 157.

[13] Humanitarian Emergency Response Africa (HERA). (2022). Nigeria COVID-19 Subnational Data. Retrieved March 3, 2024, from https://data.humdata.org/dataset/nigeria_covid19_subnational.

[14] Torres, R., Navas-Traver, I., Bibby, D., Lokas, S., Snoeij, P., Rommen, B., ... & Geudtner, D. (2017, May). Sentinel-1 SAR system and mission. In 2017 IEEE Radar Conference (RadarConf) (pp. 1582-1585). IEEE.

[15] DeVries, B., Huang, C., Armston, J., Huang, W., Jones, J. W., & Lang, M. W. (2020). Rapid and robust monitoring of flood events using Sentinel-1 and Landsat data on the Google Earth Engine. Remote Sensing of Environment, 240, 111664.

[16] Pekel, J. F., Cottam, A., Gorelick, N., & Belward, A. S. (2016). High-resolution mapping of global surface water and its long-term changes. Nature, 540(7633), 418-422.

[17] Luo, W., Xiong, C., Wan, J., Feng, Z., Ayorinde, O., Blanco, N., ... & Abimiku, A. L. (2023). Revealing human mobility trends during the SARS-CoV-2 pandemic in Nigeria via a data-driven approach. South African Journal of Science, 119(5-6), 1-9.

[18] Hersbach, H., Bell, B., Berrisford, P., Hirahara, S., Horányi, A., Muñoz‐Sabater, J., Nicolas, J., Peubey, C., Radu, R., Schepers, D. and Simmons, A., 2020. The ERA5 global reanalysis. Quarterly Journal of the Royal Meteorological Society, 146(730), pp.1999-2049.

[19] Sannigrahi, S., Pilla, F., Basu, B., Basu, A. S., & Molter, A. (2020). Examining the association between socio-demographic composition and COVID-19 fatalities in the European region using spatial regression approach. Sustainable cities and society, 62, 102418.

[20] Karmakar, M., Lantz, P. M., & Tipirneni, R. (2020). Association of social and demographic factors with COVID-19 incidence and death rates in the US. JAMA Netw Open. 2021; 4 (1): e2036462.

[21] Ezema, I. J. (2023). Availability and access to open government data in Nigeria: a content analysis of government websites and Nigerian data portal. International Information & Library Review, 55(1), 15-28.

[22] Elhorst, J.P. (2010). Spatial Panel Data Models. In: Fischer, M., Getis, A. (eds) Handbook of Applied Spatial Analysis. Springer, Berlin, Heidelberg. https://doi.org/10.1007/978-3-642-03647-7_19.

[23] Mets, K. D., Armenteras, D., & Dávalos, L. M. (2017). Spatial autocorrelation reduces model precision and predictive power in deforestation analyses. Ecosphere, 8(5), e01824.

[24] Kühn, I. (2007). Incorporating spatial autocorrelation may invert observed patterns. Diversity and Distributions, 13(1), 66-69.

[25] Legendre, P. (1993). Spatial autocorrelation: trouble or new paradigm?. Ecology, 74(6), 1659-1673.

[26] Saputro, D. R. S., Muhsinin, R. Y., & Widyaningsih, P. (2019, May). Spatial autoregressive with a spatial autoregressive error term model and its parameter estimation with two-stage generalized spatial least square procedure. In Journal of Physics: Conference Series (Vol. 1217, No. 1, p. 012104). IOP Publishing.

[27] Suryowati, K., Bekti, R. D., & Faradila, A. (2018, April). A comparison of weights matrices on computation of dengue spatial autocorrelation. In IOP Conference Series: Materials Science and Engineering (Vol. 335, No. 1, p. 012052). IOP Publishing.

[28] Baltagi, B. H., Song, S. H., & Koh, W. (2003). Testing panel data regression models with spatial error correlation. Journal of econometrics, 117(1), 123-150.

[29] Millo, G. (2011). Maximum Likelihood Estimation of Spatially and Serially Correlated Panels With Random Effects: An Estimation Framework and a Software Implementation. In Program and Abstracts (pp. 65-65). Statistical Society of Slovenia.